

Cathepsin C Inhibitors: Property Optimization and Identification of a Clinical Candidate

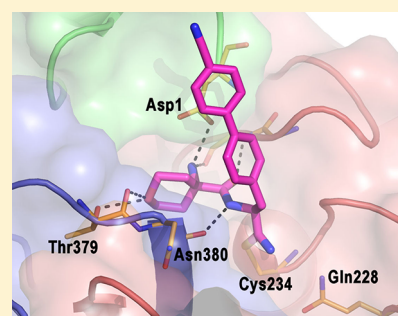
Mark Furber,^{*,†} Anna-Karin Tiden,[‡] Philip Gardiner,[†] Antonio Mete,[‡] Rhonan Ford,[‡] Ian Millichip,[‡] Linda Stein,[‡] Andrew Mather,[‡] Elizabeth Kinchin,[‡] Christopher Luckhurst,[‡] Simon Barber,[‡] Peter Cage,[‡] Hitesh Sanganeer,[§] Rupert Austin,[‡] Kamaldeep Chohan,[‡] Raj Beri,[‡] Bob Thong,[‡] Alan Wallace,[‡] Victor Oreffo,[‡] Ray Hutchinson,[‡] Steve Harper,[‡] Judit Debreczeni,[§] Jason Breed,[§] Lisa Wissler,[†] and Karl Edman[†]

[†]AstraZeneca, Pepparedsleden 1, Mölndal 431 83, Sweden

[‡]AstraZeneca, Bakewell Road, Loughborough, Leicestershire, LE11 5RH, United Kingdom

[§]AstraZeneca, Alderley Park, Cheshire, SK10 4TG, United Kingdom

ABSTRACT: A lead generation and optimization program delivered the highly selective and potent CatC inhibitor **10** as an *in vivo* tool compound and potential development candidate. Structural studies were undertaken to generate SAR understanding.



■ INTRODUCTION

Cathepsin C (CatC or dipeptidyl peptidase I) is a lysosomal cysteine protease that is important for intracellular protein degradation and plays a key role in the activation of the proinflammatory serine proteases neutrophil elastase (NE), cathepsin G (CatG), and proteinase-3 (PR-3).¹ In humans, CatC mutations are associated with the autosomal recessive disorders Haim–Munck syndrome and Papillon–Lefèvre syndrome, both associated with almost complete loss of the secondary enzymatic activities of all three serine proteases, NE, CatG, and PR-3, in neutrophils and granzyme B in NK cells and characterized by palmoplantar keratosis and severe childhood periodontal disease.^{2,3} Knockout studies in mice and pharmacological inhibition using CatC inhibitors have confirmed a central role for CatC in the activation of these granule serine proteases and strongly support the therapeutic strategy of targeting CatC inhibition in diseases such as COPD that carry a high neutrophilic burden.^{4,5} At the same time, such studies have demonstrated the need for a high degree of inhibition to demonstrate therapeutically significant effects.^{5,6}

The potential therapeutic utility and medicinal chemistry of cathepsin C have been reviewed,¹ as have attempts to develop inhibitors of this enzyme.⁷ Most known CatC inhibitors are believed to interact through covalent bond formation with the active site cysteine (Cys-234), and the electrophilic and sometimes peptidic nature of these molecules is frequently associated with poor metabolic stability while also presenting a potential safety concern because of poor selectivity and off-

target effects. Overcoming such issues is a serious hurdle, and there can be little doubt that this is the principal reason why no CatC inhibitor has progressed in clinical development so far.

A commonly used warhead in cysteine cathepsin inhibitors is the nitrile group,⁸ and a number of nitrile inhibitors of CatC have been described⁷ wherein the nitrile group traps a cysteine residue in a covalent but reversible fashion. Three chemical classes of nitriles have generally been used in such cysteine protease inhibitors: (i) cyanamides, (ii) aryl or heteroaryl nitriles, and (iii) amino- or amidoacetonitriles; these differ in their electrophilic properties. Where electrophilicity is weak (e.g., simple aryl nitriles), protease inhibition is invariably also weak. Where electrophilicity is too high (some cyanamides and heterocyclic nitriles), poor selectivity and nonspecific tissue binding can present a significant concern (e.g., irreversible binding in human liver microsomes).⁹ Amidoacetonitrile derivatives have, in some studies, shown a low potential for such nonspecific covalent binding,⁹ and Combo was the first company to describe amidoacetonitrile-based inhibitors of CatC (e.g., compound **1** in 2004).¹⁰

Understanding Cell Potency and Inhibitor Binding. In assessing amidoacetonitriles as potential start points for a medicinal chemistry program targeting CatC, the potential for lysosomotropism¹¹ was also considered given that the basic nature of some of these CatC inhibitors could result in

Received: November 5, 2013

Published: March 4, 2014

accumulation in the acidic lysosomal compartment. Although achieving higher effective concentration at the target, which is itself located within lysosomes, such effects can, in some cases, result in a loss of selectivity.¹¹ We therefore developed a cell assay to monitor this effect and to profile compounds for cell activity versus enzyme activity.¹² Interestingly, in this cellular assay, compound **1** was shown to be relatively poorly potent (pIC_{50} 7.2) despite high activity against the isolated enzyme (pIC_{50} 8.7). This is contrary to expectation for a basic compound of this type, and it indicated a potential compound stability or permeability issue. Indeed, on further investigation, compound **1** and related examples from the series were shown to be subject to rapid proteolysis in the cell assay medium, indicating a level of instability that could not be carried forward. Hydrolysis of the amide bond was shown to be enzymatic in nature because the instability could be repeated in plasma ($t_{1/2}$ rat plasma, 1.1 h; $t_{1/2}$ human plasma, 3.1 h), whereas the compounds were chemically stable at pH 2, 7.4, and 10 ($t_{1/2}$ > 100 h). Although plasma instability was viewed as problematic for a lead compound, it was anticipated this could be resolved by substitution around the amide bond, and this could form part of an initial chemistry exploration.

Alongside such a chemistry program, we wished to generate structural information to help understand SAR. The published X-ray crystal structure of human CatC reveals a tetrameric structure containing four identical subunits.¹³ Each subunit comprises three chains: light and heavy chains forming the catalytic domain, and a third chain constituting the so-called exclusion domain that blocks the active site cleft beyond the S2 pocket and is responsible for the exopeptidase activity of CatC. As reference point, the structure of compound **1** was determined in the active site of full-length human CatC. The structure of CatC in complex with compound **1** confirmed covalent interaction of the nitrile group with Cys234 and, consistent with the high enzyme activity of compound **1**, showed several putative hydrogen bonds to backbone atoms of Gly277 and Asn380 as well as to the side chain of Asp1 (Figure 1). In addition, the primary amine makes an indirect interaction to Thr379 via a water molecule in the S2 pocket.

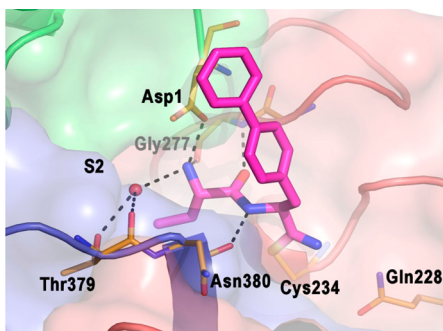
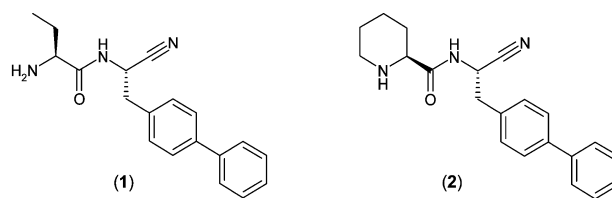


Figure 1. X-ray structure of compound **1** (magenta) bound in the active site of CatC (PDB 4cdc). The exclusion domain, heavy chain, and light chain of CatC are colored green, pink, and blue, respectively.

In an initial chemical exploration to improve plasma stability of compound **1**, piperidine derivative **2** was prepared (Figure 2). Although less potent than compound **1** in the isolated enzyme assay, **2** proved to be resistant to plasma hydrolysis (no evidence of hydrolysis in rat or human plasma after 10 h) and showed no noticeable drop-off in potency in moving from the isolated enzyme assay to the cell assay. Unfortunately, although



human CatC enzyme assay	pIC_{50} 8.7	human CatC enzyme assay	pIC_{50} 6.9
human Cat C cell assay	pIC_{50} 7.2	human Cat C cell assay	pIC_{50} 6.8

Figure 2. Initial lead structures.

having improved plasma stability, the compound had poor metabolic stability, being rapidly turned over in the presence of rat hepatocytes *in vitro*. In fact, poor metabolic stability is a feature of both compounds **1** and **2**, but, if anything, metabolic stability had decreased compared to **1** (intrinsic clearance, Cl_{int} >150 vs 91 $\mu\text{L}/\text{min}/10^6$ cells for **1** in rat hepatocytes). To understand the high metabolic clearance of this compound, a metabolite profile was determined. Compound **2** was shown by LC-MS/MS analysis to be heavily oxidized on the two phenyl rings of the biphenyl system in both rat (fresh) and human (cryopreserved) hepatocytes. Although the precise location of oxidation was not determined, it was reasoned that incorporation of electron-withdrawing substituents would reduce the propensity for oxidation. To this end, substituents were incorporated into the biphenyl to determine their effect on the ease of oxidation. This was most successful with compound **3** (Table 1) bearing a simple nitrile substituent in the 4-position of the outer phenyl ring. This simple substitution gave a promising compound because the greatly increased metabolic stability *in vitro*, accompanied by good *in vivo* PK in rat (Cl , 16 mL/min/kg; V_{ss} , 5.6 L/kg; $t_{1/2}$, 4.5 h; and bioavailability, 75%), was attended by a modest improvement in potency in both the enzyme and cell assays.

The structure of CatC in complex with compound **3** (Figure 3) revealed that the piperidine ring occupies additional space in the S2 pocket and displaces a bound water molecule from the compound **1** structure. This displacement results in loss of the indirect interaction to Thr379 and might explain the lower enzyme potency observed for compounds **2** and **3**.

Although the potency of **3** itself was not viewed as sufficient for this particular compound to progress further, the compound was viewed as providing a good start point for a lead optimization program with an initial aim of regaining the potency that had been sacrificed to achieve stability. Toward this goal, a program was initiated to vary substitution on the biphenyl further and also on the piperidine ring to seek a suitable combination of metabolic stability and high potency. Selected examples from this work are illustrated in Table 1, where it can be seen that both highly potent and metabolically stable compounds can be identified in this series.

Within Table 1, compounds **4** and **5** represent selected examples where potency could be improved by further biphenyl substitution. More interesting, however, are compounds **6** and **7**, where incorporation of a 4(*S*)-hydroxyl into the piperidine ring affords a log unit increase in enzyme potency. Although the corresponding 4(*R*) isomer was never prepared, comparison of compound **6** versus **3** and likewise isoindolone **7** versus **5** clearly illustrates the increase in potency in the isolated enzyme assay resulting from introduction of this piperidine hydroxyl group. Furthermore, the cocrystal structure of CatC complexed with compound **6** reveals that the piperidine hydroxyl mimics

Table 1. SAR of Piperidinecarboxamide Acetonitriles

Cmpd	Structure	CatC enz pIC ₅₀ ^{12,a}	CatC cell pIC ₅₀ ^{12,b}	Human mics ^c μL/min/mg	Rat heps ^c μL/min/10 ⁶ cells	hERG Ephys ^d IC ₅₀ μM	LogD	Base pKa
3		7.4 ± 0.3	8.0 ± 0.3	<4	<3	1.4	2.7	8.4
4		8.4 ± 0.2	9.0 ± 0.4	7	13	2.7	-	-
5		7.6 ± 0.1	8.1 ± 0.2	<3	5	>33	1.0	7.1
6		8.3 ± 0.1	7.9 ± 0.3	<3	4	>33	1.4	7.6
7		8.4 ± 0.1	7.4 ± 0.5	<4	<4	>33	0.5	-

^apIC₅₀ determined for rhCatC cleavage of fluorescent substrate H-Gly-Phe-AMC.¹² ^bpIC₅₀ determined for CatC cleavage of fluorescent substrate H-Gly-Phe-AFC in human THP1 cells.¹² ^cIntrinsic clearance, Cl_{int}, determined in human microsome and rat hepatocyte preparations.¹² ^dElectrophysiology (Ephys) IonWorks IC₅₀ versus hERG (human Ether-à-go-go-related gene) channels.

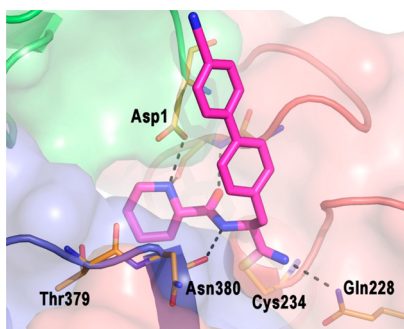


Figure 3. X-ray structure of compound 3 (magenta) bound in CatC (PDB 4cdd). The exclusion domain, heavy chain, and light chain of CatC are colored green, pink, and blue, respectively.

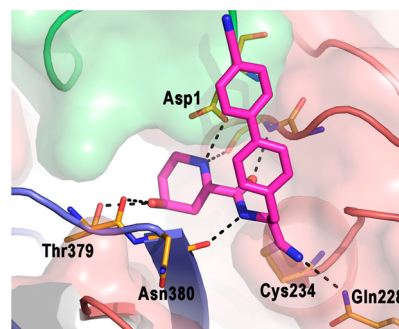


Figure 4. X-ray structure of compound 6 (magenta) bound in CatC showing the interaction of the 4(S)-hydroxyl with Thr379 (PDB 4cdf). The exclusion domain, heavy chain, and light chain of CatC are colored green, pink, and blue, respectively.

the role of a bound water molecule in the compound 1 structure, making putative interactions to both the backbone and side chain of Thr379 and thus returning a large portion of the potency lost in unsubstituted piperidines 2 and 3 (Figure 4).

Initial concerns about the weakly basic nature of compounds related to 3 and lysosomotropism proved largely unfounded because the cell potencies of all but a few compounds were generally consistent with their enzyme potencies. At the same time, compounds were profiled for activity at the hERG channel and for phospholipidosis effects in vitro. hERG data is displayed in Table 1, and it can be observed that although potentially problematic for compound 4 as well as for compound 3 itself the LogD-lowering effect of either the piperidine hydroxyl or the isindolone substituent effectively

removes this unwanted activity. Likewise, phospholipidosis effects were observed to be dependent on lipophilicity as measured by LogD, as might be anticipated for weakly basic amines. Safety profiling of compound 3 in an in vitro assay measuring phospholipid accumulation in rat hepatoma cells incubated with compound 3 (EC₅₀ 9 μM) translated into histological findings in rat in vivo studies. Significant findings were observed in liver (hypertrophy, cholangitis, vacuolation) and lung (foci of foaming macrophages), consistent with a phospholipidosis effect. In compounds 6 and 7, both basicity and overall LogD was reduced by incorporation of a hydroxyl group on the piperidine ring, and although these two compounds themselves were not studied in vivo, the in vitro

Table 2. Cathepsin Selectivity

compound	CatC Enz pIC ₅₀	CatK Enz pIC ₅₀	CatL Enz pIC ₅₀	CatS Enz pIC ₅₀	CatB Enz pIC ₅₀
3	7.4 ± 0.3	6.0 ± 0.3	<5	<5	<5
4	8.4 ± 0.2	6.4 ± 0.1	<5	<5	<5
5	7.6 ± 0.1	6.6 ± 0.1	<5	<5	<5
6	8.3 ± 0.1	5.2 ± 0.1	<5	<5	<5
7	8.4 ± 0.1	5.1 ± 0.1	<5	<5	<5

Table 3. SAR of Aminomethylenecarboxamide Acetonitriles

Cmpd	Structure	CatC Enz pIC ₅₀ ¹²	CatC Cell pIC ₅₀ ¹²	Human mics μL/min/mg	Rat heps μL/min/10 ⁶ cells	hERG Ephys IC ₅₀ μM	LogD	Base pKa
8		8.6 ± 0.1	8.5 ± 0.3	20	15	9	2.9	7.1
9		8.7 ± 0.2	7.5 ± 0.1	>150	>150	>33	2.3	5.4
10		9.0 ± 0.2	8.3 ± 0.2	3.6	2.9	26	1.9	5.8
11		9.1 ± 0.1	8.1 ± 0.2	<3	<3	>33	0.8	6.3
12		8.3 ± 0.2	7.3 ± 0.4	<3	41	>33	1.1	6.3

data for both compounds indicated a lower propensity to cause phospholipidosis (EC₅₀ 75 and > 120 μM, respectively).

An additional observation with hydroxypiperidines **6** and **7** relates to cathepsin selectivity. Given the covalent reversible nature of the interaction with CatC, we were initially concerned about cathepsin selectivity. However, from structural information, it was clear that a key interaction with CatC is the hydrogen bond between the amino group of the ligand in the S2 pocket and Asp1 of the size-exclusion domain. Because that domain is exclusive to CatC, the scope for selectivity was anticipated to be good. Indeed, as shown in Table 2, the cathepsin selectivity was generally high, with the possible exception of CatK. Introduction of the piperidine hydroxyl significantly increases the separation between CatC and CatK activity, which is in good agreement with the fact that in CatK Thr379 is replaced by a leucine residue.

In parallel to this work, a second chemical approach was undertaken to stabilize initial lead structure **1**. Following the same reasoning that instability of this compound arises because of enzymatic hydrolysis of the peptidic bond, a series of compounds was prepared wherein the α position was incorporated within a ring. Initial compounds were prepared with a cyclohexyl ring in this position (e.g., compound **8**; Table 3), and such compounds were indeed found to be stable in the cell assay and stable in plasma (both human and rat), but the potential to reintroduce lipophilicity-driven hERG and phospholipidosis effects is obvious, and some hERG activity was indeed evident in compound **8** itself. In a similar fashion to the first series of compounds, introduction of an oxygen atom

to reduce both basicity and lipophilicity, this time by incorporation within the newly introduced ring in the form of pyrans **10** and **11**, gave an improved profile, much the same effect as observed with the hydroxyl group in piperidine examples **6** and **7**. All of pyran compounds **9**–**12** displayed low Cat K activity, with only compound **12** reaching 50% inhibition at 10 μM (pIC₅₀ 5.1 for **12**).

The structure of CatC in complex with compound **10** (Figure 5) shows that the tetrahydropyran ring is positioned orthogonal to the corresponding piperidine of compound **6**. As a result, the tetrahydropyran oxygen is placed in an identical position as the piperidine hydroxyl in compound **6**. At the same

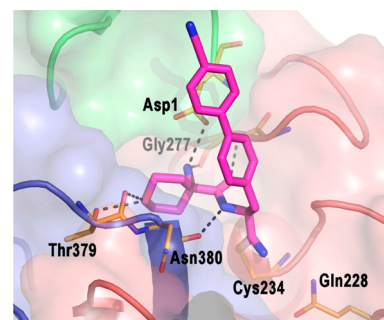
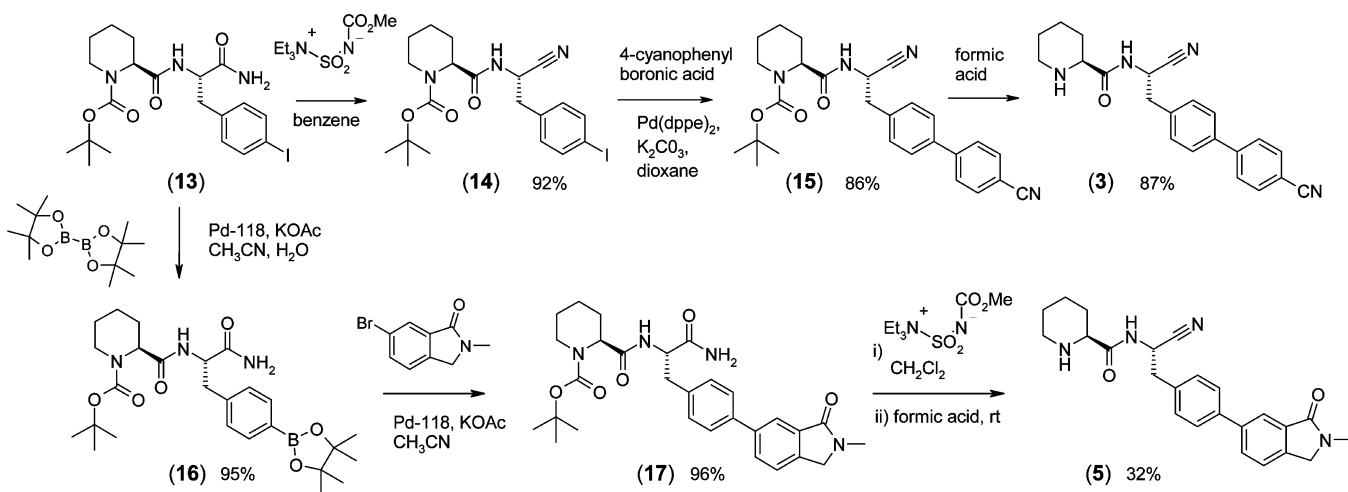
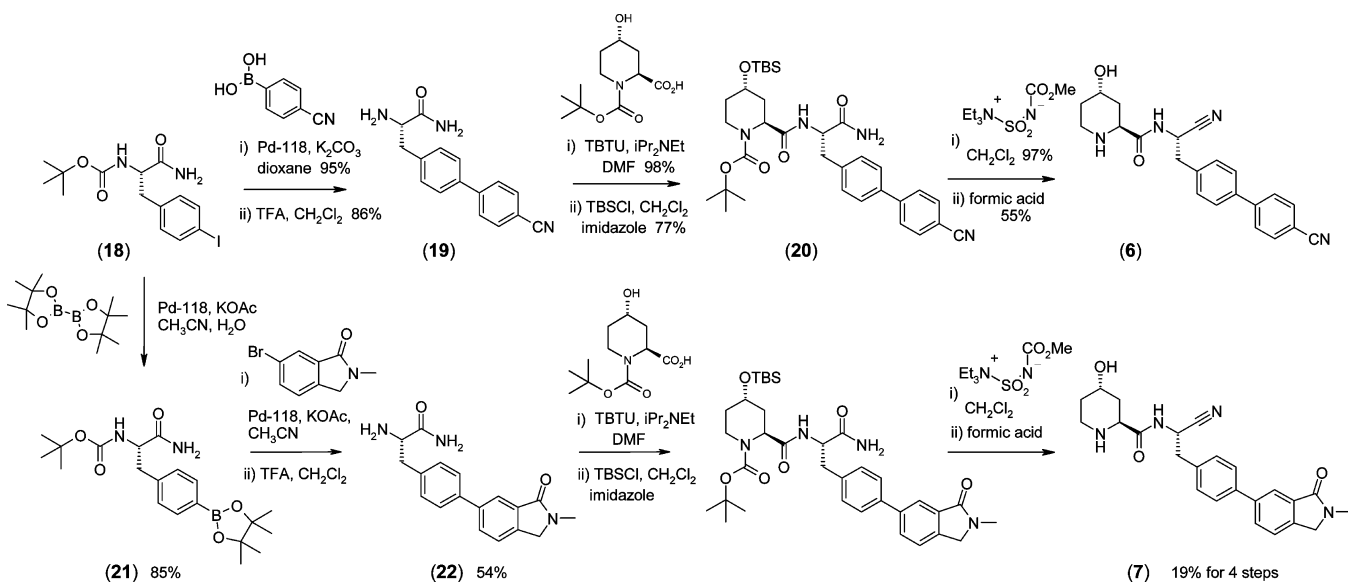


Figure 5. X-ray structure of compound **10** (magenta) bound to CatC showing how this compound also forms favorable interactions with Thr379 (PDB 4cde). The exclusion domain, heavy chain, and light chain of CatC are colored green, pink, and blue, respectively.

Scheme 1. Synthetic Scheme for the Preparation of Compounds 3 and 5

Scheme 2. Synthetic Route to 4(*S*)-Hydroxypiperidine Compounds 6 and 7

time, the primary amine is at the same position as the amine of compound **1**, donating hydrogens to interact with Asp1 and the backbone of Gly277.

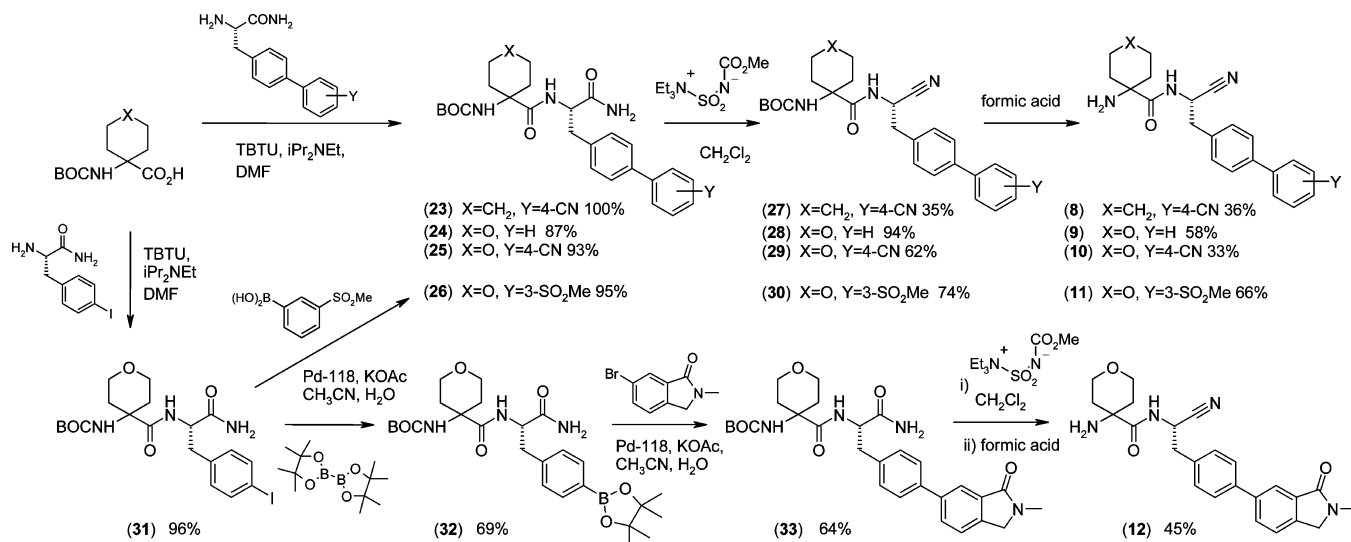
Importantly, for compounds **10** and **11**, activity at the hERG channel is also reduced, and no measurable phospholipidosis effect could be observed in *in vitro* assays. Furthermore, early *in vivo* safety profiling of compound **10** showed no observations that were ascribed to a phospholipidosis effect. An interesting observation with pyran compounds **9–12** compared to the corresponding cyclohexyl compound **8** is the finding that they display an activity drop in moving from the enzyme to the cell assay. There are several possible explanations for this observation, but one explanation is founded on the very low basicity of the amine group in such pyran compounds. The measured pK_a for compound **10** is 5.8, which is extremely low for an amine of this type compared to the measured value of 7.1 for cyclohexyl compound **8**; this is undoubtedly due, in part, to the electron-withdrawing effect of the ring oxygen. The effect of this pK_a reduction would be to reduce protonation greatly, even in the acidic environment of lysosomes, thus avoiding effects resulting from the concentration of compound within the

lysosomes. Although lysosomal accumulation of these compounds is not generally believed to be significant, it is possible that some concentration occurs for compound **8** but is absent with compounds **9–12**.

Chemistry. The preparation of compounds **3–12** was achieved using the synthetic routes illustrated in Schemes 1–3. Compounds **3** and **5** were prepared from the 4-iodophenylalanine carboxamide derivative **13**¹⁵ through either palladium-catalyzed coupling of the aryl iodide with an appropriately substituted arylboronate or through conversion of the aryl iodide itself to an arylboronate and reaction with the appropriate aryl halide (Scheme 1). Compound **4** was prepared by an analogous route to **3**.

The synthetic route to 4-hydroxypiperidine compounds **6** and **7** starting from BOC-protected (*S*)-4-iodophenylalanine carboxamide **18**²⁰ is illustrated in Scheme 2. As in Scheme 1, the aryl iodide is either coupled directly with an arylboronate in the preparation of **6** or converted itself into an arylboronate before coupling with the arylhalide; in this case, 5-bromo-2-methylisindolin-1-one for the preparation of **7**. The subsequent steps of BOC deprotection; coupling with

Scheme 3. Synthetic Route to Compounds 8–12



(2*S*,4*S*)-1-(*tert*-butoxycarbonyl)-4-hydroxypiperidine-2-carboxylic acid, hydroxyl protection, dehydration, and deprotection, are then common for the two target compounds.

The synthetic route to compounds 8–12 is illustrated in Scheme 3 starting from BOC-protected 1-amino cyclohexanecarboxylic acid or BOC-protected 4-aminotetrahydropyran-4-carboxylic acid. For preparation of 8–11, coupling with an appropriately substituted 4-arylphenylalanine carboxamide affords intermediates 23–26, and after dehydration, 27–30. Final deprotection with formic acid liberates the target compounds. Compound 12 was prepared by the alternate route of coupling BOC-protected 4-aminotetrahydropyran-4-carboxylic acid with (*S*)-4-iodophenylalanine carboxamide to afford 31 followed by conversion to arylboronate 32. Palladium-catalyzed coupling with 5-bromo-2-methylisindolin-1-one then afforded 33, which was dehydrated and deprotected to 12.

CONCLUSIONS

Compound 10 was selected as the most promising candidate as well as a potential development candidate from the compounds described for in vivo profiling on the basis of all of its measured properties. Compound 10 has low hERG activity, low activity in phospholipidosis assays ($EC_{50} > 100 \mu\text{M}$), improved selectivity versus CatK ($pIC_{50} < 5$), maintained selectivity versus CatL, CatS, and CatB ($pIC_{50} < 5$), and a clean selectivity profile in MDS Pharma screening (only a single activity >30% in >170 assays tested at 10 μM : human LTB₄ binding assay, 69% inhibition, $IC_{50} 2 \mu\text{M}$). Compound 10 also displays low clearance and high bioavailability in mouse, rat, and dog (Cl 9, 9, and 2 mL/min/kg; V_{ss} 1.6, 1.9, and 1.4 L/kg; $t_{1/2}$ 2, 3.5, and 11.6 h; bioavailability 95, 92, and 72% respectively), satisfying requirements for progression into more detailed in vivo profiling studies.

EXPERIMENTAL SECTION

Protein Production. Sf21 cells were amplified in shaker bottles to a cell density of $6.6 \times 10^6/\text{mL}$ and diluted prior to infection to $2 \times 10^6/\text{mL}$ in 10 shaker bottles (3 L) at 1000 mL working volume. The culture was infected using baculovirus stock expressing CatC (1–463) to $MOI = 2$ and then cultivated at 27 °C. Ninety-six hours postinfection, the culture was spun at 2500g for 15 min at room

temperature. Eleven liters of supernatant was collected, and CatC was activated over the weekend by adding 47 mL of papain (2 U/mL) and cysteamine to a final concentration of 5 mM, pH ~6.5. The activation was performed during slow mixing at ~10 °C. Ammonium sulfate was added to 1.8 M and EDTA to 5 mM. The pH was then adjusted to 4.5 by adding citric acid (1 M solution) followed by 20 min of stirring. The precipitated media was centrifuged at 15 900g for ~1.5 h (JLA 8.1000, 15 °C) followed by filtration. The sample was loaded onto a HIC column (butyl sepharose FF, 200 mL XK 50) overnight. The column was previously equilibrated with buffer (1.8 M $(\text{NH}_4)_2\text{SO}_4$, 20 mM citric acid, 5 mM EDTA, 5 mM cysteamine, and 0.1 M NaCl, pH 4.5). The unbound sample was washed out from the HIC column until the UV signal was less than 45 mAU (~3 cv). A 0–100% buffer (20 mM citric acid, 5 mM EDTA, 5 mM cysteamine, and 0.1 M NaCl, pH 4.5) gradient during five column volumes was applied, and relevant fractions were pooled according to activity analysis. The buffer was exchanged on the pooled CatC fractions to 10 mM Tris-HCl, 1 mM EDTA, and 5 mM cysteamine, pH 7.6. The buffer exchange was performed on a Sephadex G-25 XK 50 column (column volume 200 mL) in two consecutive runs. The buffer-exchanged HIC eluate was applied to 10 mL Q-Sepharose FF (two 5 mL Hightrap columns). The columns were previously equilibrated with 10 mM Tris-HCl, 1 mM EDTA, and 5 mM cysteamine, pH 7.6. The unbound sample was washed out from the IEX column during a washing step. A 0–50% buffer (10 mM Tris-HCl, 1 mM EDTA, 5 mM cysteamine, and 1 M NaCl, pH 7.6) gradient was applied followed by a step elution with 100% buffer before relevant fractions were collected for activity analysis. The IEX pool was loaded onto a SEC column (Superdex 200 pg, 980 mL XK 50), which was previously equilibrated with 20 mM Tris-HCl, 200 mM NaCl, and 5 mM cysteamine, pH 7.6. Relevant fractions were collected for analysis. The SEC pool was concentrated to 27 mL using a Centricon plus-80 (30 kDa cutoff). The protein concentration on the concentrated SEC pool was measured by Bradford assay to 2.5 mg/mL (67.5 mg protein). All purifications steps were performed at room temperature.

Crystallization and Structure Determination. To aid crystallization, protein buffer was exchanged to 20 mM sodium acetate, pH 5, 0.2 M sodium chloride, 0.5 mM EDTA, and 2 mM DTT with a NAP10 column (GE Healthcare). The protein sample was concentrated to 12 mg/mL. DTT and compound were added to a final concentration of 2 mM, and the sample was incubated for 30 min. Crystals were grown at 20 °C in sitting drops using 0.3 μL of protein and 0.3 μL of well solution (21–27% PEG3350, 0.2 M ammonium sulfate, and 0.1 M sodium acetate, pH 5.0). Crystals appeared after a few hours but continued to grow for a few days. Crystals were frozen in liquid nitrogen prior to data collection using 20% glycerol and well

solution as cryo protectant. X-ray diffraction data were collected at the European Synchrotron Radiation Facility (ESRF; Grenoble, France). Data were integrated and processed using MOSFLM and SCALA of the CCP4 suite.¹⁴ The crystals belonged to the space groups $P3_12_1$ or $P3_1$ with two or four molecules in the asymmetric unit. The structures were solved by molecular replacement using Protein Data Bank (PDB) entry 1K3B as the search model.¹³ The structures were refined using the CCP4 suite and manual rebuilding using Coot.¹⁵ Figures 1, 3, 4, and 5 were prepared using PyMOL.¹⁶ Crystallographic coordinates and structure factor amplitudes for all complex structures were deposited into the Protein Data Bank (accession codes 4cdc, 4cdd, 4cde, and 4cdf).

Fluorescence Assay Procedure Using Recombinant Human (rh) CatC. The activity of CatC was determined by measuring the enzymatic release of aminomethyl coumarin (AMC) from the peptide substrate (H-Gly-Arg-AMC), which leads to an increase in fluorescence intensity at $\lambda_{\text{ex}} = 350$ nm and $\lambda_{\text{em}} = 450$ nm. The assay was carried out in black 384-well plates in a final volume of 50 μL at 22 °C. The assay conditions contained the following: 25 mM piperazine buffer, pH 5.0, 50 mM NaCl, 5 mM DTT, 0.01% (v/v) Triton X100, 100 μM H-Gly-Arg-AMC, and rhCatC (~50 pM). Potential inhibitors were prepared in DMSO and then diluted in the assay to give a final concentration not exceeding 1% (v/v) DMSO. A ten-point half-log dilution series of the inhibitors (highest concentration typically 10 μM) was tested, and the pIC_{50} was determined using a four-parameter logistic equation in a non-fifteen linear curve fitting routine. A standard vinyl sulfone CatC inhibitor¹² was used as a positive control in the assay. Routinely, inhibitors were preincubated with rhCatC for 30 min prior to the addition of the peptide substrate to start the reaction for a further 60 min at 22 °C. Afterward, the plates were immediately read in a fluorescence plate reader using the above emission and excitation wavelengths (modified from refs 17 and 18).

SYNTHESIS

Reagents were obtained from commercial suppliers and used without purification. Unless otherwise stated, reactions were carried out at ambient temperature (18–25 °C) and under positive nitrogen pressure with magnetic stirring. Flash chromatography was performed on E. Merck 230–400 mesh silica gel 60 or by using Biotage KP-Sil SNAP cartridges. Solvent mixtures used as eluants are volume/volume ratios. Preparative HPLC purifications were performed on Waters Symmetry, Novapak, or XTerra columns eluting with a gradient of acetonitrile or methanol in aqueous ammonium acetate, ammonia, or trifluoroacetic acid solution. Routine ¹H and ¹³C NMR spectra were recorded on a Varian UnityInova spectrometer at a proton frequency of 300 or 400 MHz or a Bruker Avance III spectrometer at a proton frequency of 500 MHz. Chemical shifts are expressed in ppm. Low-resolution mass spectra were measured on an Agilent 1100 MSD G1946D spectrometer using electrospray (ESI) ionization, atmospheric pressure chemical ionization, or Agilent multimode ionization; only ions that indicate the parent mass or a common fragment are reported. High-resolution mass spectra were recorded on a Waters LCTP time-of-flight instrument using ESI ionization. The purity of all test compounds was determined by RPHPLC conducted on an Agilent 1100 LCMS system using UV detection and a gradient of 5–95% acetonitrile in either aqueous ammonium acetate (0.1% w/v) or trifluoroacetic acid (0.1% v/v) over 2.5 min on 2.1 mm × 5 mm columns packed with Waters Symmetry C8 or Waters Symmetry C18 or on 2.0 mm × 50 mm columns packed with Phenomenex Max-RP. All test compounds showed ≥95% purity.

(S)-N-((S)-1-Cyano-2-(biphenyl-4-yl)ethyl)piperidine-2-carboxamide (2).¹⁹ ¹H NMR (399.8 MHz, DMSO-*d*₆) δ 9.23 (d, *J* = 10.3 Hz, 1H), 7.65–7.61 (m, 4H), 7.43 (m, 4H), 7.36 (m, 1H), 5.01 (q, *J* = 7.5 Hz, 1H), 4.29 (s, 1H), 3.80 (d, *J* = 13.6 Hz, 1H), 3.28–3.19 (m, 3H), 2.96–2.89 (m, 1H), 2.49 (t, *J* = 2.6 Hz, 2H), 2.09 (m, 1H), 1.80–1.45 (m, 3H). HRMS (ESI) *m/z* calcd for C₂₁H₂₃N₃O (M + H)⁺, 334.1919; found, 334.1945.

(S)-tert-Butyl-2-((S)-1-cyano-2-(4-iodophenyl)ethylcarbamoyl)piperidine-1-carboxylate (14). Triethylamine (11.73 mL, 84.12 mmol) in benzene (20 mL) was stirred under

nitrogen in a cold water bath, and methyl chlorosulfonylcarbamate (5.70 g, 32.86 mmol) in benzene (60 mL) was added dropwise. Once addition was complete, the cold water bath was removed, and the mixture was stirred at room temperature for 30 min. A solution of (S)-tert-butyl 2-((S)-1-amino-3-(4-iodophenyl)-1-oxopropan-2-ylcarbamoyl)piperidine-1-carboxylate (13)¹⁹ (6.59 g, 13.14 mmol) in benzene (50 mL) was added dropwise, and the mixture was stirred at room temperature for 2 h. Water was added to the reaction mixture, and the organic phase was isolated, washed with brine, dried (MgSO₄), filtered, and concentrated in vacuo. The crude product was purified by flash silica chromatography eluting with 20% ethyl acetate in isohexane. Pure fractions were evaporated to dryness to give compound 14 (5.86 g, 92%) as a white solid.

(S)-tert-Butyl-2-((S)-1-cyano-2-(4'-cyanobiphenyl-4-yl)ethylcarbamoyl)piperidine-1-carboxylate (15). (S)-tert-Butyl 2-((S)-1-cyano-2-(4-iodophenyl)ethylcarbamoyl)piperidine-1-carboxylate (14) (8.5 g, 17.59 mmol) and bis[1,2-bis(diphenylphosphino)ethane]palladium (0.159 g, 0.18 mmol) were stirred in dioxane, and to the mixture was added 4-cyanophenylboronic acid (3.88 g, 26.38 mmol). The reaction mixture was stirred under nitrogen for 15 min, and then 2 M aqueous potassium carbonate solution (17.59 mL, 35.17 mmol) was added. The reaction mixture was heated at 75 °C overnight. LCMS showed that the reaction was complete. After cooling to room temperature, the reaction mixture was split and poured onto Chem Elut cartridges (Agilent), and the crude product was washed through with CH₂Cl₂. The combined solvent was removed in vacuo, and the crude material obtained was purified by flash silica chromatography eluting with 25% ethyl acetate in isohexane to give compound 15 (6.90 g, 86%) as a colorless solid. ¹H NMR (399.8 MHz, DMSO-*d*₆) δ 8.64 (d, *J* = 7.7 Hz, 1H), 7.92 (dd, *J* = 6.5 and 1.9 Hz, 2H), 7.86 (d, *J* = 8.5 Hz, 2H), 7.71 (d, *J* = 8.2 Hz, 2H), 7.44 (d, *J* = 8.2 Hz, 2H), 5.14–5.06 (m, 1H), 4.62–4.35 (m, 1H), 3.78–3.70 (m, 1H), 3.26–3.15 (m, 2H), 2.85 (td, *J* = 13.0 and 3.0 Hz, 1H), 2.00–1.87 (m, 1H), 1.55–1.16 (m, 13H), 1.06–0.94 (m, 1H).

(S)-N-((S)-1-Cyano-2-(4'-cyanobiphenyl-4-yl)ethyl)piperidine-2-carboxamide (3). (S)-tert-Butyl-2-((S)-1-cyano-2-(4'-cyanobiphenyl-4-yl)ethylcarbamoyl)piperidine-1-carboxylate (15) (2.8 g, 6.11 mmol) was dissolved in formic acid (25 mL, 651.81 mmol), and the solution was heated at 50 °C for 10 min. Solvent was removed in vacuo, and the crude product was purified by preparative HPLC using a 95–5% gradient of aqueous 0.1% trifluoroacetic acid in acetonitrile as eluent. The fractions containing the desired compound were concentrated in vacuo to afford compound 3 as the trifluoroacetate salt (2.50 g, 87%). ¹H NMR (399.8 MHz, DMSO-*d*₆) δ 8.51 (d, *J* = 7.6 Hz, 1H), 7.89 (m, 4H), 7.72 (d, *J* = 8.0 Hz, 2H), 7.44 (d, *J* = 8.0 Hz, 2H), 5.03 (m, 1H), 3.20 (m, 2H), 3.06 (m, 1H), 2.78 (m, 1H), 2.45 (m, 1H), 1.57 (m, 2H), 1.42–1.19 (m, 4H). ¹³C NMR (125.8 MHz, DMSO-*d*₆) δ 173.28, 144.15, 136.85, 136.40, 132.76, 130.14, 127.31, 126.91, 119.14, 118.77, 109.86, 58.91, 44.68, 36.63, 29.00, 25.53, 23.44. HRMS (ESI) *m/z* calcd for C₂₂H₂₂N₄O (M + H)⁺, 359.1872; found, 359.1886.

(S)-N-((S)-1-Cyano-2-(4'-cyano-3'-(methylthio)biphenyl-4-yl)ethyl)piperidine-2-carboxamide (4).¹⁹ ¹H NMR (399.8 MHz, DMSO-*d*₆) δ 9.29 (d, *J* = 7.2 Hz, 1H), 9.01–8.69 (m, 1H), 7.81 (d, *J* = 7.9 Hz, 1H), 7.78 (t, *J* = 7.8 Hz), 7.64–7.56 (m, 2H), 7.47 (d, *J* = 8.2 Hz, 2H), 5.07 (q, *J* = 7.4 Hz, 1H), 3.82–3.71 (m, 2H), 3.28–3.17 (m, 3H), 2.98–2.86 (m, 1H), 2.70 (s, 3H), 2.10–0.00 (m, 1H), 1.82–1.74 (m, 1H), 1.73–1.65 (m, 1H), 1.64–1.42 (m, 2H). ¹³C NMR (125.8 MHz, DMSO-*d*₆) δ 168.85, 144.66, 143.92, 137.15, 136.16, 134.06, 130.19, 127.34, 123.43, 123.30, 118.50, 116.88, 108.04, 56.48, 43.20, 41.80, 36.31, 26.67, 21.38, 14.34. HRMS (ESI) *m/z* calcd for C₂₃H₂₄N₄OS (M + H)⁺, 405.1749; found, 405.1761.

(S)-tert-Butyl-2-((S)-1-amino-1-oxo-3-(4-(4,4,5,5-tetramethyl-1,3,2-dioxaborolan-2-yl)phenyl)propan-2-ylcarbamoyl)piperidine-1-carboxylate (16). A solution of (S)-tert-butyl-2-((S)-1-amino-3-(4-iodophenyl)-1-oxopropan-2-ylcarbamoyl)piperidine-1-carboxylate (13)¹⁹ (21.7 g, 43.28 mmol) in acetonitrile (250 mL) was treated with potassium acetate (12.74 g, 129.85 mmol) and 4,4',4',5,5',5'-octamethyl-2,2'-bis(1,3,2-dioxaborolane) (14.62 g, 57.57 mmol). Water (15 mL) was added followed by Pd-118 (30

mg, 0.05 mmol), and the mixture was stirred under nitrogen at 95 °C for 17 h. The cooled reaction mixture was concentrated to low volume, and the residue was partitioned between water (500 mL) and ether (2 × 500 mL). The ethereal phase was collected and dried over magnesium sulfate and filtered. The filtrate was passed through a pad of flash silica gel product eluting with diethyl ether then with ethyl acetate. The ethyl acetate solution was concentrated to dryness to afford compound **16** (20.5 g, 95%) as a colorless solid. ¹H NMR (399.8 MHz, CDCl₃) δ 7.75 (d, *J* = 7.9 Hz, 2H), 7.24 (d, *J* = 7.9 Hz, 2H), 6.48–6.39 (m, 1H), 5.30–5.23 (m, 1H), 4.72 (q, *J* = 7.6 Hz, 1H), 4.76–4.62 (m, 1H), 3.22–3.14 (m, 1H), 3.13–3.06 (m, 1H), 2.48–2.36 (m, 1H), 2.25–2.18 (m, 1H), 1.53–1.45 (m, 4H), 1.42 (s, 9H), 1.33 (s, 12H). MS [M-BOC + H]⁺ = 402.

(S)-tert-Butyl-2-((S)-1-amino-3-(4-(2-methyl-1-oxoisindolin-5-yl)phenyl)-1-oxopropan-2-ylcarbamoyl)piperidine-1-carboxylate (17). A solution of (S)-tert-butyl-2-((S)-1-amino-1-oxo-3-(4-(4,4,5,5-tetramethyl-1,3,2-dioxaborolan-2-yl)phenyl)propan-2-ylcarbamoyl)piperidine-1-carboxylate (**16**) (300 mg, 0.60 mmol), potassium acetate (176 mg, 1.79 mmol), and 5-bromo-2-methylisindolin-1-one (271 mg, 1.20 mmol) in acetonitrile (30 mL) under a nitrogen atmosphere was treated with Pd-118 (11.70 mg, 0.02 mmol), and the mixture was heated at 80 °C for 3 h. The solvent was removed in vacuo, and the residue was purified on silica gel eluting with ethyl acetate followed by methanol to afford compound **17** (300 mg, 96%) as a gum. ¹H NMR (399.8 MHz, CDCl₃) δ 7.88 (d, *J* = 7.7 Hz, 1H), 7.62 (dd, *J* = 7.9 and 1.5 Hz, 1H), 7.59 (s, 1H), 7.56 (dd, *J* = 6.5 and 1.7 Hz, 2H), 7.33 (d, *J* = 8.2 Hz, 2H), 6.54 (d, *J* = 7.7 Hz, 1H), 6.20–6.05 (m, 1H), 5.51 (s, 1H), 4.80 (q, *J* = 7.8 Hz, 1H), 4.69–4.65 (m, 1H), 4.43 (s, 2H), 3.92–3.74 (m, 1H), 3.27–3.10 (m, 6H), 2.49–2.32 (m, 1H), 2.24–2.17 (m, 1H), 1.61–1.25 (m, 15H includes H₂O peak). MS [M - H]⁻ = 520.

(S)-N-((S)-1-Cyano-2-(4-(2-methyl-1-oxoisindolin-5-yl)phenyl)ethyl)piperidine-2-carboxamide (5). A solution of (S)-tert-butyl-2-((S)-1-amino-3-(4-(2-methyl-1-oxoisindolin-5-yl)phenyl)-1-oxopropan-2-ylcarbamoyl)piperidine-1-carboxylate (**17**) (300 mg, 0.58 mmol) and methyl *N*-(triethylammoniumsulfonyl)carbamate (412 mg, 1.73 mmol) in CH₂Cl₂ (15 mL) was stirred at room temperature for 20 h. The reaction mixture was placed on a flash silica column, and the mixture eluted with 70% ether/isohexane to afford a gum (200 mg) (MS [M + H-tBu]⁺ = 448, MS [M - H]⁻ = 502), which was dissolved in formic acid (1 mL, 26.07 mmol) and then stirred at room temperature for 4 h. The mixture was then concentrated to dryness, and the residue was purified on reversed-phase HPLC (aq 0.1% TFA/MeCN). The fractions were freeze-dried to afford compound **5** (65.0 mg, 31.6%) as a colorless solid. ¹H NMR (399.8 MHz, DMSO-*d*₆) δ 9.31 (d, *J* = 7.4 Hz, 1H), 9.01–8.92 (m, 1H), 8.81–8.68 (m, 1H), 7.87 (s, 1H), 7.79–7.69 (m, 4H), 7.45 (d, *J* = 8.2 Hz, 2H), 5.07 (q, *J* = 7.5 Hz, 1H), 4.52 (s, 2H), 3.82–3.73 (m, 1H), 3.27–3.18 (m, 3H), 3.10 (s, 3H), 2.99–2.86 (m, 1H), 2.10–2.02 (m, 1H), 1.82–1.42 (m, 5H). ¹³C NMR (125.8 MHz, DMSO-*d*₆) δ 168.85, 166.99, 142.60, 142.53, 138.48, 135.14, 131.56, 130.14, 127.09, 126.39, 123.04, 121.39, 56.48, 51.43, 43.20, 41.81, 36.30, 28.99, 26.67, 21.39, 21.14. HRMS (ESI) *m/z* calcd for C₂₄H₂₆N₄O₂ (M + H)⁺, 403.2134; found, 403.2142.

(S)-tert-Butyl-1-amino-3-(4-iodophenyl)-1-oxopropan-2-ylcarbamate (18). To a solution of (S)-2-(tert-butoxycarbonylamino)-3-(4-iodophenyl)propanoic acid²⁰ (2.05 g, 5.24 mmol) in DMF (15 mL) was added *N*-ethylmorpholine (0.995 mL, 7.86 mmol) followed by TBTU (1.683 g, 5.24 mmol). The mixture was stirred at room temperature for 30 min and then cooled to 0 °C. Aqueous ammonia (35%, 0.580 mL, 10.48 mmol) was added, and the mixture was allowed to reach room temperature and stirred overnight. The reaction mixture was poured into water (150 mL), and the resulting suspension was filtered. The solid was dried in vacuo to afford compound **18** (1.910 g, 93%) as an off-white solid, which was used without further purification. ¹H NMR (399.8 MHz, CDCl₃) δ 7.63 (d, *J* = 8.5 Hz, 2H), 6.98 (d, *J* = 8.5 Hz, 2H), 5.89 (s, 1H), 5.45 (s, 1H), 5.02 (s, 1H), 4.34 (s, 1H), 3.05–2.98 (m, 2H), 1.41 (s, 9H).

(S)-2-Amino-3-(4'-cyanobiphenyl-4-yl)propanamide (19). A solution of (S)-tert-butyl-1-amino-3-(4-iodophenyl)-1-oxopropan-2-

ylcarbamate (**18**) (3.17 g, 8.12 mmol) and 4-cyanophenylboronic acid (1.194 g, 8.12 mmol) in dioxane (5 mL) was treated with Pd-118 (0.080 g, 0.12 mmol), and the mixture was stirred at room temperature for 15 min under nitrogen. An aqueous solution of potassium carbonate (8.12 mL, 16.25 mmol) was added, and the mixture was stirred for 18 h at 75 °C. LCMS demonstrated complete reaction, and the product was extracted into ethyl acetate, dried, and evaporated to afford (S)-tert-butyl-1-amino-3-(4'-cyanobiphenyl-4-yl)-1-oxopropan-2-ylcarbamate (3.13 g), which was used without further purification in the next step. ¹H NMR (399.8 MHz, CDCl₃) δ 7.72 (d, *J* = 8.7 Hz, 2H), 7.66 (d, *J* = 8.7 Hz, 2H), 7.54 (d, *J* = 7.9 Hz, 2H), 7.35 (d, *J* = 7.9 Hz, 2H), 5.90–5.83 (m, 1H), 5.42–5.34 (m, 1H), 5.10–5.01 (m, 1H), 4.48–4.37 (m, 1H), 3.21–3.07 (m, 2H), 1.42 (s, 9H).

To a solution of (S)-tert-butyl-1-amino-3-(4'-cyanobiphenyl-4-yl)-1-oxopropan-2-ylcarbamate (3.13 g, 8.57 mmol) in CH₂Cl₂ (30 mL) was added TFA (1.32 mL, 17.13 mmol). The CH₂Cl₂ was distilled off on a rotary evaporator at atmospheric pressure to leave a few milliliters of solvent. The reaction was monitored by HPLC/MS, and when it was complete, it was partitioned between water and CH₂Cl₂, dried, and evaporated. The solid was purified on silica eluting with ethyl acetate and then ethyl acetate containing 10% methanol to afford compound **19** (1.95 g, 86%). ¹H NMR (399.8 MHz, CDCl₃) δ 7.73 (dd, *J* = 6.7 and 2.1 Hz, 2H), 7.67 (dd, *J* = 6.4 and 2.1 Hz, 2H), 7.56 (dt, *J* = 8.0 and 1.7 Hz, 2H), 7.36 (dt, *J* = 8.4 and 2.1 Hz, 2H), 7.11 (s, 1H), 5.38 (s, 1H), 3.68 (dd, *J* = 9.1 and 4.2 Hz, 1H), 3.32 (dd, *J* = 13.8 and 4.1 Hz, 1H), 2.84 (dd, *J* = 13.8 and 9.2 Hz, 1H), 1.49 (s, 2H). MS (M + H)⁺ = 266.

(2S,4S)-tert-Butyl-2-((S)-1-amino-3-(4'-cyanobiphenyl-4-yl)-1-oxopropan-2-ylcarbamoyl)-4-(tert-butylidimethylsilyloxy)piperidine-1-carboxylate (20). To a solution of (2S,4S)-1-(tert-butoxycarbonyl)-4-hydroxypiperidine-2-carboxylic acid (**19**) (157 mg, 0.64 mmol) and (S)-2-amino-3-(4'-cyanobiphenyl-4-yl)propanamide (170 mg, 0.64 mmol) in DMF (5 mL) was added Hünig's base (0.279 mL, 1.60 mmol) followed by TBTU (308 mg, 0.96 mmol). The resulting solution was stirred at room temperature for 2 h and then poured into water (50 mL) and extracted with CH₂Cl₂ (2 × 50 mL). The organics were dried (magnesium sulfate) and evaporated in vacuo to afford crude (2S,4S)-tert-butyl-2-((S)-1-amino-3-(4'-cyanobiphenyl-4-yl)-1-oxopropan-2-ylcarbamoyl)-4-hydroxypiperidine-1-carboxylate (310 mg, 0.63 mmol, 98%) as a brown gum. This gum was dissolved in CH₂Cl₂ (10 mL), and imidazole (107 mg, 1.57 mmol) and tert-butylidimethylsilyl chloride (104 mg, 0.69 mmol) were added under nitrogen. The resulting solution was stirred at room temperature for 24 h. The reaction was diluted with further CH₂Cl₂ (50 mL) and washed with water (2 × 50 mL). The organics were dried (magnesium sulfate) and evaporated in vacuo, and the residue was purified by flash silica chromatography eluting with 60% ethyl acetate in isohexane. Pure fractions were evaporated to dryness to afford compound **20** (294 mg, 77%) as a white foam. ¹H NMR (399.8 MHz, CDCl₃) δ 7.73 (d, *J* = 8.0 Hz, 2H), 7.65 (d, *J* = 8.0 Hz, 2H), 7.54 (d, *J* = 8.4 Hz, 2H), 7.33 (d, *J* = 8.4 Hz, 2H), 6.58 (d, *J* = 8.6 Hz, 1H), 6.11–5.92 (m, 1H), 5.44 (s, 1H), 4.80–4.71 (m, 2H), 3.91–3.66 (m, 2H), 3.24 (dd, *J* = 14.0 and 6.8 Hz, 1H), 3.09 (dd, *J* = 14.0 and 6.8 Hz, 1H), 2.32 (d, *J* = 13.5 Hz, 2H), 1.66 (s, 2H), 1.58 (d, *J* = 12.9 Hz, 1H), 1.43 (s, 9H), 0.85 (s, 9H), 0.03 (d, *J* = 6.4 Hz, 6H). MS [M - H]⁻ = 605.

(2S,4S)-N-((S)-1-Cyano-2-(4'-cyanobiphenyl-4-yl)ethyl)-4-hydroxypiperidine-2-carboxamide (6). A solution of (2S,4S)-tert-butyl-2-((S)-1-amino-3-(4'-cyanobiphenyl-4-yl)-1-oxopropan-2-ylcarbamoyl)-4-(tert-butylidimethylsilyloxy)piperidine-1-carboxylate (**20**) (290 mg, 0.48 mmol) in CH₂Cl₂ (10 mL) was treated with methyl *N*-(triethylammoniumsulfonyl)carbamate (148 mg, 0.62 mmol) and stirred at room temperature overnight. The reaction was evaporated in vacuo, and the residue was purified by flash silica chromatography eluting with 20% ethyl acetate in isohexane. Pure fractions were evaporated to dryness to afford (2S,4S)-tert-butyl-4-(tert-butylidimethylsilyloxy)-2-((S)-1-cyano-2-(4'-cyanobiphenyl-4-yl)-ethylcarbamoyl)piperidine-1-carboxylate (272 mg, 97%) as a colorless gum. ¹H NMR (399.8 MHz, CDCl₃) δ 7.74 (d, *J* = 8.1 Hz, 2H), 7.66 (d, *J* = 8.1 Hz, 2H), 7.58 (d, *J* = 8.4 Hz, 2H), 7.37 (d, *J* = 8.4 Hz, 2H),

5.17 (s, 1H), 4.78 (s, 1H), 4.02–3.83 (m, 1H), 3.19–3.08 (m, 2H), 2.56–2.24 (m, 2H), 1.66 (d, $J = 14.3$ Hz, 1H), 1.51–1.30 (m, 13H), 0.87 (s, 9H), 0.06 (d, $J = 5.9$ Hz, 6H).

A solution of (2*S*,4*S*)-*tert*-butyl-4-(*tert*-butyldimethylsilyloxy)-2-((*S*)-1-cyano-2-(4'-cyanobiphenyl-4-yl)ethylcarbamoyl)piperidine-1-carboxylate (250 mg, 0.42 mmol) in formic acid (5 mL) was stirred at 50 °C for 30 min. The reaction was poured onto ice (50 mL), basified to pH 9 with concentrated aqueous ammonia, and extracted with CH₂Cl₂ (2 × 50 mL). The organics were dried (sodium sulfate) and evaporated in vacuo. The residue was dissolved in dry tetrahydrofuran (5 mL) and treated with TBAF (1 M in THF) (0.425 mL, 0.42 mmol). The reaction was stirred at room temperature overnight, diluted with water (100 mL), and extracted with CH₂Cl₂ (3 × 100 mL). The organics were dried (sodium sulfate) and evaporated in vacuo, and the residue was purified by preparative HPLC using a 95–5% gradient of aqueous 0.1% trifluoroacetic acid in methanol as eluent. Fractions containing the desired compound were combined, and the methanol was removed in vacuo. The aqueous residue was basified with saturated sodium bicarbonate solution and extracted with ethyl acetate (2 × 50 mL). The organics were dried (sodium sulfate) and evaporated in vacuo to afford compound **6** (88 mg, 55%) as a white solid. ¹H NMR (399.8 MHz, CDCl₃) δ 7.74 (d, $J = 8.4$ Hz, 2H), 7.67 (d, $J = 8.4$ Hz, 2H), 7.62 (s, 1H), 7.59 (d, $J = 8.1$ Hz, 2H), 7.40 (d, $J = 8.1$ Hz, 2H), 5.18 (q, $J = 8.0$ Hz, 1H), 3.87–3.80 (m, 1H), 3.70 (dd, $J = 7.2$ Hz, $J = 4.4$ Hz, 1H), 3.29–3.22 (m, 1H), 3.18 (d, $J = 7.2$ Hz, 2H), 3.05–2.97 (m, 1H), 2.58–2.49 (m, 1H), 2.08–1.99 (m, 1H), 1.73–1.54 (m, 2H), 1.48–1.39 (m, 2H). HRMS (ESI) m/z calcd for C₂₂H₂₂N₄O₂ (M + H)⁺, 375.1821; found, 375.1812.

(*S*)-*tert*-Butyl-1-amino-1-oxo-3-(4-(4,4,5,5-tetramethyl-1,3,2-dioxaborolan-2-yl)phenyl)propan-2-ylcarbamate (21). A mixture of (*S*)-*tert*-butyl-1-amino-3-(4-iodophenyl)-1-oxopropan-2-ylcarbamate (**18**) (1 g, 2.56 mmol), 4,4,4',4',5,5,5',5'-octamethyl-2,2'-bi(1,3,2-dioxaborolane) (0.781 g, 3.08 mmol), potassium acetate (0.503 g, 5.13 mmol), and Pd-118 (0.05 g, 0.08 mmol) in aqueous acetonitrile (30 mL, 1:1) under nitrogen was heated at reflux for 11 h. The reaction mixture was diluted with water (100 mL), and the products were extracted into ethyl acetate (100 mL). The extracts were dried over magnesium sulfate and concentrated to an oil. The crude product was purified on silica gel eluting with ethyl acetate to give compound **21** (850 mg, 85%) as a gum, which slowly solidified. ¹H NMR (399.8 MHz, CDCl₃) δ 7.72 (d, $J = 8.0$ Hz, 2H), 7.22 (d, $J = 8.0$ Hz, 2H), 5.66 (m, 1H), 5.30 (m, 1H), 5.04 (m, 1H), 4.33 (m, 1H), 5.18 (q, $J = 8.0$ Hz, 1H), 3.14–3.09 (m, 1H), 3.09–2.98 (m, 1H), 1.59 (s, 6H), 1.31 (s, 9H), 1.21 (s, 6H). MS (M + H-BOC)⁺ = 291.

(*S*)-2-Amino-3-(4-(2-methyl-1-oxoisindolin-5-yl)phenyl)propanamide (22). A mixture of (*S*)-*tert*-butyl-1-amino-1-oxo-3-(4-(4,4,5,5-tetramethyl-1,3,2-dioxaborolan-2-yl)phenyl)propan-2-ylcarbamate (**21**) (850 mg, 2.18 mmol), potassium acetate (427 mg, 4.36 mmol), 5-bromo-2-methylisindolin-1-one (650 mg, 2.88 mmol), and Pd-118 (42.6 mg, 0.07 mmol) in a mixture of water (15 mL) and acetonitrile (25 mL) under a nitrogen atmosphere was stirred and heated under reflux for 6 h. The reaction mixture was concentrated to dryness, and the residue was treated with TFA (10 mL, 129.80 mmol) and heated at 60 °C for 15 min. Excess TFA was removed in vacuo, and the residue was quenched with a saturated aqueous sodium bicarbonate solution. The mixture was extracted with ethyl acetate (2 × 100 mL), which only extracted out unreacted starting materials. The aqueous phase was repeatedly extracted with *n*-butanol until no additional product could be extracted from the aqueous phase (~200 mL). The butanol extract was concentrated to dryness, and the residue was triturated with methanol (20 mL). The suspension was concentrated to a viscous oil, which was purified by reversed-phase HPLC (70–10% 0.1% aqueous TFA/methanol) to afford compound **22** (TFA salt, 500 mg, 54.2%) as colorless solid. ¹H NMR (399.8 MHz, DMSO-*d*₆) δ 8.19–8.08 (m, 3H), 7.91–7.86 (m, 2H), 7.79–7.71 (m, 4H), 7.61 (s, 1H), 7.40 (d, $J = 8.2$ Hz, 2H), 4.52 (s, 2H), 4.00 (s, 1H), 3.19–2.98 (m, 5H). MS (M + H)⁺ = 310.

(2*S*,4*S*)-*N*-((*S*)-1-Cyano-2-(4-(2-methyl-1-oxoisindolin-5-yl)phenyl)ethyl)-4-hydroxypiperidine-2-carboxamide (7). To a solution of (2*S*,4*S*)-1-(*tert*-butoxycarbonyl)-4-hydroxypiperidine-2-car-

boxylic acid (190 mg, 0.77 mmol) and (*S*)-2-amino-3-(4-(2-methyl-1-oxoisindolin-5-yl)phenyl)propanamide (**22**) (361 mg, 0.85 mmol) in DMF (5 mL) was added Hünig's base (0.474 mL, 2.71 mmol) followed by TBTU (298 mg, 0.93 mmol). The resulting solution was stirred at room temperature for 72 h, poured into water (50 mL), and extracted with CH₂Cl₂ (2 × 50 mL). The organics were dried (magnesium sulfate), evaporated in vacuo, and purified on silica gel using 85% ethyl acetate/methanol as eluant to afford (2*S*,4*S*)-*tert*-butyl-2-((*S*)-1-amino-3-(4-(2-methyl-1-oxoisindolin-5-yl)phenyl)-1-oxopropan-2-ylcarbamoyl)-4-hydroxypiperidine-1-carboxylate (530 mg) as a gum, which was progressed directly into the next reaction without further characterization. A solution of (2*S*,4*S*)-*tert*-butyl-2-((*S*)-1-amino-3-(4-(2-methyl-1-oxoisindolin-5-yl)phenyl)-1-oxopropan-2-ylcarbamoyl)-4-hydroxypiperidine-1-carboxylate (530 mmol) in CH₂Cl₂ (25 mL) was treated with imidazole (67.2 mg, 0.99 mmol) and TBDMS-Cl (149 mg, 0.99 mmol), and the mixture was stirred overnight. LC/MS showed complete conversion to silylated product, and the mixture was concentrated to dryness. The residue was purified on silica gel by initial elution with ether and then ethyl acetate to afford a low-melting solid; 500 mg was progressed directly into the next reaction. MS (M + H-BOC)⁺ = 511. A solution of (2*S*,4*S*)-*tert*-butyl-2-((*S*)-1-amino-3-(4-(2-methyl-1-oxoisindolin-5-yl)phenyl)-1-oxopropan-2-ylcarbamoyl)-4-(*tert*-butyldimethylsilyloxy)piperidine-1-carboxylate (500 mg, 0.77 mmol) in CH₂Cl₂ (20 mL) was stirred with methyl *N*-(triethylammoniumsulfonyl)carbamate (366 mg, 1.54 mmol) overnight. The solvent was removed in vacuo, and the residue was treated with formic acid (10 mL, 260.73 mmol). After 4 h at room temperature, the reaction mixture was concentrated to dryness. The residue was basified with a saturated aqueous sodium bicarbonate solution, and the precipitated product was extracted into ethyl acetate (2 × 100 mL). The combined extracts were dried over magnesium sulfate and concentrated to dryness to afford a gum, which was purified by HPLC (0.1% aq ammonia/MeOH, 950S, X-Bridge) to give compound **7** (60 mg, 19% yield over four chemical steps) as a colorless solid. ¹H NMR (500.3 MHz, CDCl₃) δ 7.89 (d, $J = 7.9$ Hz, 1H), 7.69–7.55 (m, 4H), 7.42–7.34 (m, 2H), 5.18 (t, $J = 7.0$ Hz, 1H), 4.43 (s, 2H), 3.88–3.81 (m, 1H), 3.71–3.65 (m, 1H), 3.47 (s, 1H), 3.25–3.13 (m, 5H), 3.03–2.95 (m, 1H), 2.57–2.49 (m, 1H), 2.02–1.95 (m, 1H), 1.72–1.61 (m, 2H), 1.48–1.40 (m, 1H). HRMS (ESI) m/z calcd for C₂₄H₂₆N₄O₃ (M + H)⁺, 419.2083; found, 419.2076.

(*S*)-*tert*-Butyl-1-(1-amino-3-(4'-cyanobiphenyl-4-yl)-1-oxopropan-2-ylcarbamoyl)cyclohexylcarbamate (23). To a solution of (*S*)-2-amino-3-(4'-cyanobiphenyl-4-yl)propanamide²⁰ (300 mg, 1.13 mmol) and 1-(*tert*-butoxycarbonylamino)cyclohexanecarboxylic acid (275 mg, 1.13 mmol) in DMF (5 mL) was added triethylamine (0.394 mL, 2.83 mmol) followed by TBTU (545 mg, 1.70 mmol). The mixture was stirred at room temperature for 2 h. The mixture was poured into water and diethyl ether (20 mL), and the mixture was separated. The aqueous layer was further extracted with diethyl ether, and the combined organic extracts were dried over magnesium sulfate. The residue after evaporation was purified by chromatography on silica eluting with methanol/CH₂Cl₂/Et₃N 10:90:1 to give compound **23** (561 mg, 100%). MS [M + H]⁺ = 491, [M + H-BOC]⁺ 391.6.

(*S*)-*tert*-Butyl-1-(1-cyano-2-(4'-cyanobiphenyl-4-yl)-ethylcarbamoyl)cyclohexylcarbamate (27). To a solution of (*S*)-*tert*-butyl-1-(1-amino-3-(4'-cyanobiphenyl-4-yl)-1-oxopropan-2-ylcarbamoyl)cyclohexylcarbamate (**23**) (550 mg, 1.12 mmol) in CH₂Cl₂ (3 mL) was added methyl *N*-(triethylammoniumsulfonyl)carbamate (321 mg, 1.35 mmol), and the mixture was stirred overnight. The mixture was poured into water (10 mL) and extracted with CH₂Cl₂ (2 × 5 mL). The combined organic layers were dried (Mg₂SO₄) and evaporated to dryness. Recrystallization from ethyl acetate/isohexane afforded compound **27** (185 mg, 34.9%) as a white solid, which was collected by filtration and dried in vacuo. ¹H NMR (399.8 MHz, DMSO-*d*₆) δ 8.04 (d, $J = 8.2$ Hz, 1H), 7.90–7.81 (m, 4H), 7.68 (d, $J = 8.2$ Hz, 2H), 7.43 (d, $J = 8.2$ Hz, 2H), 6.18 (s, 1H), 5.01 (q, $J = 7.9$ Hz, 1H), 3.24–3.09 (m, 2H), 1.86–1.40 (m, 8H), 1.37 (s, 9H), 1.31–1.11 (m, 2H).

(*S*)-1-Amino-*N*-(1-cyano-2-(4'-cyanobiphenyl-4-yl)ethyl)-cyclohexanecarboxamide (8). To (*S*)-*tert*-butyl-1-(1-cyano-2-(4'-

cyanobiphenyl-4-yl)ethylcarbamoyl)cyclohexylcarbamate (27) (160 mg, 0.34 mmol) was added formic acid (1.5 mL, 39.11 mmol), and the mixture was stirred for 2 h. The mixture was poured into water and neutralized with 880 ammonia. The aqueous phase was extracted with diethyl ether (3 × 10 mL), and the combined organics were dried over magnesium sulfate. The crude oil was diluted with methanol (2 mL) and purified by preparative chromatography eluting with 25–85% acetonitrile containing 0.1% TFA to give compound 8 (60.0 mg, 36.4%) as a white solid. ¹H NMR (399.8 MHz, DMSO-*d*₆) δ 9.14 (d, *J* = 7.9 Hz, 1H), 8.17 (s, 2H), 7.93 (d, *J* = 9.4 Hz, 2H), 7.87 (d, *J* = 8.3 Hz, 2H), 7.73 (d, *J* = 8.2 Hz, 2H), 7.44 (d, *J* = 8.2 Hz, 2H), 5.16–5.08 (m, 1H), 3.32–3.18 (m, 2H), 1.99–1.87 (m, 1H), 1.85–1.75 (m, 1H), 1.75–1.65 (m, 1H), 1.62–1.40 (m, 6H), 1.34–1.19 (m, 1H), 1.376 (s, 1H). ¹³C NMR (125.8 MHz, DMSO-*d*₆) δ 171.33, 144.12, 137.06, 136.11, 132.85, 130.29, 127.38, 126.99, 118.82, 118.80, 110.00, 59.52, 41.78, 36.50, 30.69, 30.29, 23.59, 19.67. HRMS (ESI) *m/z* calcd. for C₂₃H₂₄N₄O (M + H)⁺, 373.2028; found, 373.2016.

(S)-4-Amino-N-(2-(biphenyl-4-yl)-1-cyanoethyl)tetrahydro-2H-pyran-4-carboxamide (9). ¹H NMR (500.3 MHz, CDCl₃) δ 8.15 (d, *J* = 9.0 Hz, 1H), 7.53–7.49 (m, 4H), 7.40–7.35 (m, 2H), 7.31–7.25 (m, 3H), 5.06 (dt, *J* = 9.0 Hz, *J* = 6.8 Hz, 1H), 3.87–3.76 (m, 2H), 3.52 (dtd, *J* = 13.6, 11.5, and 2.3 Hz, 2H), 3.08 (q, *J* = 7.0 Hz, 2H), 2.22 (ddd, *J* = 13.9, 11.1, and 4.7 Hz, 1H), 2.10 (ddd, *J* = 13.8, 11.1, and 4.7 Hz, 1H), 1.24–1.19 (m, 1H), 1.13–1.08 (m, 1H). ¹³C NMR (125.8 MHz, DMSO-*d*₆) δ 176.96, 139.75, 138.87, 134.88, 130.02, 128.89, 127.36, 126.55, 126.52, 119.33, 62.46, 62.31, 54.37, 41.29, 36.81, 34.63, 34.53. HRMS (ESI) *m/z* calcd for C₂₁H₂₃N₃O₂ (M + H)⁺, 350.1868; found, 350.1875.

(S)-tert-Butyl-4-(1-amino-3-(4'-cyanobiphenyl-4-yl)-1-oxopropan-2-ylcarbamoyl)tetrahydro-2H-pyran-4-ylcarbamate (25). To a solution of 4-(*tert*-butoxycarbonylamino)tetrahydro-2H-pyran-4-carboxylic acid (374 mg, 1.52 mmol), (S)-2-amino-3-(4'-cyanobiphenyl-4-yl)propanamide, ²⁰ (405 mg, 1.52 mmol) and *N*-ethyl-*N*-isopropylpropan-2-amine (0.664 mL, 3.81 mmol) in DMF (10 mL) was added TBTU (734 mg, 2.29 mmol), and the reaction mixture was stirred at room temperature for 48 h. The reaction mixture was evaporated to dryness, dissolved in CH₂Cl₂ (20 mL), and evaporated onto silica. The silica was placed on the top of a silica column and eluted with 20% ethyl acetate in isohexane, with 50% ethyl acetate in isohexane, and then with 100% ethyl acetate to afford, after concentration in vacuo, compound 25 (700 mg, 93%) as a colorless solid. ¹H NMR (399.8 MHz, CDCl₃) δ 7.73 (dt, *J* = 8.5 and 1.7 Hz, 2H), 7.67 (dt, *J* = 8.4 and 1.7 Hz, 2H), 7.58 (dt, *J* = 8.4 and 2.0 Hz, 2H), 7.42 (d, *J* = 8.2 Hz, 2H), 5.14 (dd, *J* = 14.4 and 7.2 Hz, 1H), 4.87 (s, 1H), 3.74–3.57 (m, 2H), 3.21–3.11 (m, 8H), 1.84 (s, 0.67H), 1.80 (s, 0.33H), 1.43 (s, 6H), 1.43 (s, 3H). [M + H-BOC]⁺ = 393.

(S)-tert-Butyl-4-(1-cyano-2-(4'-cyanobiphenyl-4-yl)ethylcarbamoyl)tetrahydro-2H-pyran-4-ylcarbamate (29). To a solution of (S)-*tert*-butyl-4-(1-amino-3-(4'-cyanobiphenyl-4-yl)-1-oxopropan-2-ylcarbamoyl)tetrahydro-2H-pyran-4-ylcarbamate (25) (0.70 g) in CH₂Cl₂ (15 mL) was added methyl *N*-(triethylammoniumsulfonyl)carbamate (0.356 g), and the mixture was stirred at room temperature for 6 h. Additional methyl *N*-(triethylammoniumsulfonyl)carbamate (0.15 g) was added, and the mixture was stirred overnight. The mixture was absorbed onto silica and purified by chromatography on silica eluting with 33% ethyl acetate in isohexane and then with 100% ethyl acetate to afford compound 29 (0.42 g) as a colorless solid. ¹H NMR (399.8 MHz, CDCl₃) δ 7.74 (d, *J* = 8.5 Hz, 2H), 7.67 (d, *J* = 8.6 Hz, 2H), 7.59 (d, *J* = 8.2 Hz, 2H), 7.42 (d, *J* = 8.2 Hz, 2H), 5.14 (dd, *J* = 15.2 and 7.6 Hz, 1H), 4.70 (s, 1H), 3.83–3.76 (m, 1H), 3.75–3.66 (m, 1H), 3.66–3.56 (m, 2H), 3.17 (dd, *J* = 13.5 and 6.2 Hz, 1H), 3.12 (dd, *J* = 14.0 and 7.8 Hz, 1H), 2.28–1.86 (m, 4H), 1.85–1.77 (m, 1H), 1.44 (s, 9H). MS [M – H][–] = 473.

(S)-4-Amino-N-(1-cyano-2-(4'-cyanobiphenyl-4-yl)ethyl)tetrahydro-2H-pyran-4-carboxamide (10). To (S)-*tert*-butyl-4-(1-cyano-2-(4'-cyanobiphenyl-4-yl)ethylcarbamoyl) tetrahydro-2H-pyran-4-ylcarbamate (29) (420 mg) was added formic acid (2 mL), and the mixture was heated to 50 °C for 10 min. The mixture was evaporated to dryness, dissolved in methanol (4 mL), and purified

by reverse-phase HPLC eluting with 25–85% acetonitrile containing 0.1% TFA. Fractions containing product were concentrated in vacuo to remove acetonitrile, neutralized with a saturated sodium bicarbonate solution, and extracted with CH₂Cl₂, which was then dried and concentrated in vacuo to give compound 10 (110 mg) as a colorless solid. Anal. Calcd for C₂₂H₂₂N₄O₂: C, 70.57; H, 5.92; N, 14.96. Found: C, 70.32; H, 5.99; N, 14.87. ¹H NMR (500.3 MHz, DMSO-*d*₆) δ 7.92 (d, *J* = 8.4 Hz, 2H), 7.87 (d, *J* = 8.4 Hz, 2H), 7.71 (d, *J* = 8.2 Hz, 2H), 7.43 (d, *J* = 8.2 Hz, 2H), 5.02 (t, *J* = 7.8 Hz, 1H), 3.65–3.54 (m, 3H), 3.45 (dt, *J* = 11.9 and 4.3 Hz, 1H), 3.32 (s, 2H), 3.26–3.16 (m, 2H), 1.89 (ddd, *J* = 13.4, 10.5, and 4.8 Hz, 1H), 1.73 (ddd, *J* = 13.4, 10.8, and 4.5 Hz, 1H), 1.21 (dq, *J* = 13.4 and 2.7 Hz, 1H), 1.12 (dq, *J* = 13.4 and 2.4 Hz, 1H). ¹³C NMR (125.8 MHz, DMSO-*d*₆) δ 176.91, 144.14, 136.84, 136.38, 132.76, 130.20, 127.31, 126.89, 119.23, 118.77, 109.86, 62.38, 62.22, 54.29, 41.09, 36.71, 34.56, 34.45. EE determination by chiral HPLC purity 98.2% at 275 nm. HRMS (ESI) *m/z* calcd for C₂₂H₂₂N₄O₂ (M + H)⁺, 375.1821; found, 375.1841.

(S)-4-Amino-N-(1-cyano-2-(3'-(methylsulfonyl)biphenyl-4-yl)ethyl)tetrahydro-2H-pyran-4-carboxamide (11). ²⁰ ¹H NMR (399.8 MHz, DMSO-*d*₆) δ 9.24 (d, *J* = 7.9 Hz, 1H), 8.44 (s, 3H), 8.13 (t, *J* = 1.8 Hz, 1H), 8.02 (dt, *J* = 8.0 and 1.4 Hz, 1H), 7.92 (dt, *J* = 8.0 and 1.2 Hz, 1H), 7.77–7.72 (m, 3H), 7.47 (d, *J* = 8.4 Hz, 2H), 5.19–5.12 (m, 1H), 3.71–3.63 (m, 2H), 3.63–3.55 (m, 2H), 3.29 (s, 3H), 3.33–3.18 (m, 2H), 2.24–2.14 (m, 1H), 2.09–1.99 (m, 1H), 1.69 (d, *J* = 14.1 Hz, 1H), 1.48 (d, *J* = 13.8 Hz, 1H). ¹³C NMR (125.8 MHz, DMSO-*d*₆) δ 176.08, 141.65, 140.82137.30, 135.61, 131.55, 130.23, 130.11, 126.96, 124.74, 61.35, 56.99, 43.41, 41.87, 30.46, 30.92, 36.43. HRMS (ESI) *m/z* calcd for C₂₂H₂₅N₃O₄S (M + H)⁺, 428.1644; found, 428.1680.

(S)-tert-Butyl-4-(1-amino-3-(4-iodophenyl)-1-oxopropan-2-ylcarbamoyl)tetrahydro-2H-pyran-4-ylcarbamate (31). 4-(*tert*-Butoxycarbonylamino)tetrahydro-2H-pyran-4-carboxylic acid (3.14 g, 12.79 mmol), (S)-2-amino-3-(4-iodophenyl)propanamide (3.71 g, 12.79 mmol), and *N*-ethyl-*N*-isopropylpropan-2-amine (5.57 mL, 31.97 mmol) were dissolved in DMF (10 mL), and to the solution was added TBTU (5.34 g, 16.63 mmol). The reaction mixture was stirred overnight at room temperature. The reaction mixture was evaporated to dryness, dissolved in CH₂Cl₂ (40 mL), and evaporated onto silica. The silica was placed on the top of a silica column and eluted with 50% ethyl acetate in isohexane and then with 100% ethyl acetate to give compound 31 (6.33 g, 96%). ¹H NMR (399.8 MHz, CDCl₃) δ 7.62 (d, *J* = 8.2 Hz, 2H), 6.96 (d, *J* = 8.5 Hz, 2H), 6.88 (s, 1H), 6.51 (d, *J* = 6.7 Hz, 1H), 5.38 (s, 1H), 5.00 (s, 1H), 4.73 (dd, *J* = 14.7 and 6.5 Hz, 1H), 3.87 (dt, *J* = 11.8 and 4.4 Hz, 1H), 3.70 (dt, *J* = 11.9 and 4.2 Hz, 1H), 3.56 (t, *J* = 10.7 Hz, 2H), 3.21–3.08 (m, 2H), 2.28 (ddd, *J* = 14.1, 10.0, and 4.2 Hz, 1H), 1.89 (ddd, *J* = 13.7, 9.9, and 4.0 Hz, 1H), 1.81 (d, *J* = 14.1 Hz, 1H), 1.58 (d, *J* = 13.6 Hz, 1H), 1.36 (s, 9H). [M + 2H-*t*Bu]⁺ = 418.0.

(S)-tert-Butyl-4-(1-amino-1-oxo-3-(4-(4,4,5,5-tetramethyl-1,3,2-dioxaborolan-2-yl)phenyl)propan-2-ylcarbamoyl)tetrahydro-2H-pyran-4-ylcarbamate (32). A mixture of 4,4,4',4',5,5,5',5'-octamethyl-2,2'-bi(1,3,2-dioxaborolane) (1.576 g, 6.21 mmol), (S)-*tert*-butyl-4-(1-amino-3-(4-iodophenyl)-1-oxopropan-2-ylcarbamoyl)tetrahydro-2H-pyran-4-ylcarbamate (31) (2.47 g, 4.77 mmol), and potassium acetate (1.406 g, 14.32 mmol) in acetonitrile (50 mL) and water (8 mL) was treated with Pd-118 (50 mg, 0.08 mmol) under a nitrogen atmosphere, and the mixture was stirred and heated under reflux for 24 h. Further potassium acetate (0.352 g, 3.58 mmol), 4,4,4',4',5,5,5',5'-octamethyl-2,2'-bi(1,3,2-dioxaborolane) (0.394 g, 1.55 mmol), and Pd-118 (50 mg, 0.08 mmol) were added, and heating was continued for an additional 24 h. The reaction was evaporated in vacuo, and the residue was partitioned between ethyl acetate (200 mL) and water (200 mL). The organics were dried (magnesium sulfate) and evaporated in vacuo, and the crude product was purified by flash silica chromatography eluting with ethyl acetate. Pure fractions were evaporated to dryness to give compound 32 (1.710 g, 69.2%) as a pale brown foam. ¹H NMR (399.8 MHz, CDCl₃) δ 7.74 (d, *J* = 7.7 Hz, 2H), 7.21 (d, *J* = 7.7 Hz, 2H), 6.82 (s, 1H), 6.43 (m, 1H), 5.32 (s, 1H), 4.92 (s, 1H), 4.73 (q, *J* = 7.2

Hz, 1H), 3.87 (dt, $J = 12.4$ and 4.6 Hz, 1H), 3.68 (dt, $J = 12.4$ and 4.6 Hz, 1H), 3.59–3.48 (m, 2H), 3.30–3.12 (m, 2H), 2.35–2.25 (m, 1H), 1.91–1.77 (m, 2H), 1.56–1.49 (m, 1H), 1.33 (d, $J = 2.3$ Hz, 12H), 1.24 (s, 9H).

(S)-tert-Butyl-4-(1-amino-3-(4-(2-methyl-3-oxoisindolin-5-yl)phenyl)-1-oxopropan-2-ylcarbamoyl)tetrahydro-2H-pyran-4-ylcarbamate (33). (S)-tert-Butyl-4-(1-amino-1-oxo-3-(4-(4,4,5,5-tetramethyl-1,3,2-dioxaborolan-2-yl)phenyl)propan-2-ylcarbamoyl)-tetrahydro-2H-pyran-4-ylcarbamate (32) (300 mg, 0.58 mmol), 6-bromo-2-methylisindolin-1-one (131 mg, 0.58 mmol), and potassium acetate (171 mg, 1.74 mmol) in a mixture of acetonitrile (15 mL) and water (5 mL) were stirred under nitrogen at 90 °C with Pd-118 (378 mg, 0.58 mmol). After 4 h, the reaction was judged to be complete, affording one major product. The reaction mixture was cooled to room temperature and diluted with water (50 mL). The products were extracted with ethyl acetate (3 × 50 mL), and the combined extracts were dried and concentrated to give compound 33 as a gum (200 mg). $[M + H-BOC]^+ = 436.9$.

(S)-4-Amino-N-(1-cyano-2-(4-(2-methyl-3-oxoisindolin-5-yl)phenyl)ethyl)tetrahydro-2H-pyran-4-carboxamide (12). (S)-tert-Butyl-4-(1-amino-3-(4-(2-methyl-3-oxoisindolin-5-yl)phenyl)-1-oxopropan-2-ylcarbamoyl)tetrahydro-2H-pyran-4-ylcarbamate (33) (200 mg, 0.37 mmol) in CH_2Cl_2 (20 mL) was stirred at room temperature with methyl N-(triethylammonium)sulfonylcarbamate (178 mg, 0.75 mmol) for 20 h. The reaction mixture was concentrated to dryness, and the residue was stirred at room temperature in formic acid (0.5 mL, 13.04 mmol) for 2 h to affect deprotection. The solution was diluted with water (20 mL) and basified with 880 ammonia solution. The products were extracted into ethyl acetate (100 mL), and the extract was dried over magnesium sulfate. Concentration afforded a gum, which was purified by reversed-phase chromatography (0.1% aq TFA/methanol, 70–30%). The product-containing fractions were freeze-dried to give compound 12 (TFA salt, 90 mg, 45.3%) as a colorless solid. 1H NMR (500.3 MHz, D_2O) δ 7.60–7.56 (m, 2H), 7.44 (d, $J = 10.2$ Hz, 2H), 7.38 (d, $J = 7.7$ Hz, 1H), 7.28 (d, $J = 10.2$ Hz, 2H), 5.17 (dd, $J = 9.5$ and 6.7 Hz, 1H), 4.25 (s, 2H), 3.70–3.53 (m, 3H), 3.43–3.37 (m, 1H), 3.31 (dd, $J = 13.9$ and 6.6 Hz, 1H), 3.16 (dd, $J = 13.8$ and 9.7 Hz, 1H), 2.99 (s, 3H), 2.20–2.12 (m, 1H), 2.05–1.97 (m, 1H), 1.86–1.80 (m, 1H), 1.68–1.61 (m, 1H). HRMS (ESI) m/z calcd for $C_{24}H_{27}N_4O_3$ (M + H) $^+$, 419.2083; found, 419.2085.

AUTHOR INFORMATION

Corresponding Author

*E-mail: mark1.furber@astrazeneca.com.

Notes

The authors declare no competing financial interest.

ACKNOWLEDGMENTS

We thank Richard Weaver and Cathy MacDonald for providing DMPK support, Theresa Humphries for synthesis support, and Marie Castaldo for assistance with protein production methods.

ABBREVIATIONS USED

TBTU, N,N,N',N' -tetramethyl-*O*-(benzotriazol-1-yl)uronium tetrafluoroborate; Pd-118, 1,1-bis(di-*tert*-butylphosphino)-ferrocene palladium dichloride; Cl, clearance; V_{ss} , apparent steady-state volume of distribution; $t_{1/2}$, half-life

REFERENCES

- (1) Guay, D.; Beaulieu, C.; Percival, M. D. Therapeutic utility and medicinal chemistry of cathepsin C inhibitors. *Curr. Top. Med. Chem.* **2010**, *10*, 708–716.
- (2) Hart, T. C.; Hart, P. S.; Michalec, M. D.; Zhang, Y.; Firatli, E.; Van Dyke, T. E.; Stabholz, A.; Zlotogorski, A.; Shapira, L.; Soskolne, W. A. Haim-Munk syndrome and Papillon-Lefèvre syndrome are allelic mutations in Cathepsin C. *J. Med. Genet.* **2000**, *37*, 88–94.

- (3) Pham, C. T.; Ivanovich, J. L.; Raptis, S. Z.; Zehnbauser, B.; Ley, T. J. Papillon-Lefèvre syndrome: Correlating the molecular, cellular and clinical consequences of cathepsin C deficiency in humans. *J. Immunol.* **2004**, *173*, 7277–7281.

- (4) Adkinson, A. M.; Raptis, S. Z.; Kelley, D. G.; Pham, C. T. Dipeptidylpeptidase I activates neutrophil-derived serine proteases and regulates the development of acute experimental arthritis. *J. Clin. Invest.* **2002**, *109*, 363–371.

- (5) Methot, N.; Rubin, J.; Guay, D.; Beaulieu, C.; Ethier, D.; Jagadeeswarar, R., T.; Reindeau, D.; Percival, M. D. Inhibition of the activation of multiple serine proteases with a cathepsin C inhibitor requires sustained exposure to prevent proenzyme processing. *J. Biol. Chem.* **2007**, *282*, 20836–20846.

- (6) Methot, N.; Guay, D.; Rubin, J.; Ethier, D.; Ortega, K.; Wong, S.; Normandin, D.; Beaulieu, C.; Reddy, T. J.; Reindeau, D.; Percival, M. D. In vivo inhibition of serine protease processing requires a high fractional inhibition of cathepsin C. *Mol. Pharmacol.* **2008**, *73*, 1857–1865.

- (7) Laine, D. I.; Busch-Petersen, J. Inhibitors of cathepsin C. *Expert Opin. Ther. Pat.* **2010**, *20*, 497–506.

- (8) Frizler, M.; Stirnberg, M.; Sisay, M. T.; Gütschow, M. Development of nitrile-based peptidic inhibitors of cysteine cathepsins. *Curr. Top. Med. Chem.* **2010**, *10*, 294–322.

- (9) Oballa, R. M.; Truchon, J.-F.; Bayly, C. I.; Chauret, N.; Day, S.; Crane, S.; Berthelette, C. A generally applicable method for assessing the electrophilicity and reactivity of diverse nitrile compounds. *Bioorg. Med. Chem. Lett.* **2007**, *17*, 998–1002.

- (10) Bondebjerg, J.; Fuglsang, H.; Valeur, K. R.; Pedersen, J.; Naeerum, L. Dipeptidyl nitriles as human dipeptidyl peptidase I inhibitors. *Bioorg. Med. Chem. Lett.* **2006**, *16*, 3614–3617.

- (11) Black, C. W.; Percival, M. D. The consequences of lysosomotropism on the design of selective cathepsin K inhibitors. *ChemBioChem.* **2006**, *7*, 1525–1535.

- (12) Thong, B.; Pilling, J.; Ainscow, E.; Beri, R.; Unitt, J. Development and validation of a simple cell-based fluorescence assay for dipeptidyl peptidase I (DPP1) activity. *J. Biomol. Screening* **2011**, *16*, 36–43.

- (13) Turk, D.; Janvic, I.; Stern, M.; Podobnik, D.; Lamba, D.; Dahl, S. W.; Lauritzen, C.; Pedersen, J.; Turk, B. Structure of human dipeptidyl peptidase I: Exclusion domain added to an endopeptidase framework creates the machine for activation of granular serine proteases. *EMBO J.* **2001**, *20*, 6570–6582.

- (14) Collaborative Computational Project. The CCP4 suite: Programs for protein crystallography. *Acta Crystallogr., Sect. D: Biol. Crystallogr.* **1994**, *50*, 760–763.

- (15) Emsley, P.; Lohkamp, B.; Scott, W. G.; Cowtan, K. Features and development of COOT. *Acta Crystallogr., Sect. D: Biol. Crystallogr.* **2010**, *66*, 486–501.

- (16) DeLano, W. L. *The PyMOL molecular graphics system*; DeLano Scientific: San Carlos, CA, 2001.

- (17) Kam, C. M.; Gotz, M. G.; Koot, G.; McGuire, M.; Thiele, D. L.; Hudig, D.; Powers, J. C. Design and evaluation of inhibitors for dipeptidyl peptidase I (cathepsin C). *Arch. Biochem. Biophys.* **2004**, *427*, 123–134.

- (18) McGuire, M. J.; Lipsky, P. E.; Thiele, D. L. Purification and characterization of dipeptidyl peptidase I from human spleen. *Arch. Biochem. Biophys.* **1992**, *295*, 280–288.

- (19) Cage, P. A.; Furber, M.; Luckhurst, C. A.; Sangane, H. J.; Stein, L. A. Peptidyl nitriles and use thereof as dipeptidyl peptidase I inhibitors. Patent WO2009/074829.

- (20) Ford, R.; Mete, A.; Mather, A.; Millichip, I. Substituted 1-cyanoethylheterocyclic carboxamide compounds. Patent WO2010/128324.